INSTITUTE OF PHYSICS PUBLISHING SUPERCONDUCTOR SCIENCE AND TECHNOLOGY
Supercond. Sci. Technol. **19** (2006) S280–S283 doi:10.1088/0953-2048/19/5/S24

A food contaminant detection system based on high-T_c SQUIDs

Saburo Tanaka[1], **H Fujita**[1], **Y Hatsukade**[1], **T Nagaishi**[2], **K Nishi**[2], **H Ota**[2], **T Otani**[3] **and S Suzuki**[3]

[1] Toyohashi University of Technology, 1-1 Hibarigaoka Tempaku-cho Toyohashi Aichi 441-8580, Japan
[2] Sumitomo Electric Hightechs Co., Ltd, Itami, Hyogo 664-0016, Japan
[3] Advance Food Technology Co., Ltd, Toyohashi, Aichi 441-8113, Japan

Received 20 September 2005, in final form 22 November 2005
Published 6 March 2006
Online at stacks.iop.org/SUST/19/S280

Abstract
We have designed and constructed a computer controlled food contaminant detection system for practical use, based on high-T_c SQUID detectors. The system, which features waterproof stainless steel construction, is acceptable under the HACCP (Hazard Analysis and Critical Control Point) programme guidelines. The outer dimensions of the system are 1500 mm length × 477 mm width × 1445 mm height, and it can accept objects up to 200 mm wide × 80 mm high. An automatic liquid nitrogen filling system was installed in the standard model. This system employed a double-layered permeable metallic shield with a thickness of 1 mm as a magnetically shielded box. The distribution of the magnetic field in the box was simulated by FEM; the gap between each shield layer was optimized before fabrication. A shielding factor of 732 in the Z-component was achieved. This value is high enough to safely operate the system in a non-laboratory environment, i.e., a factory. During testing, we successfully detected a steel contaminant as small as 0.3 mm in diameter at a distance of 75 mm.

1. Introduction

The consumption of processed foods is a common feature of daily life. Although great efforts are made to prevent contamination during food processing, the possibility remains that contaminants may be accidentally mixed with food products. Examples of these contaminants include small metal chips or fine wires from a strainer element of a processing machine, and broken syringe needles from immunizations or hormone injections that may remain in the meat of food animals. Because of the increase in international concern regarding food safety, there is a clear need to develop a highly sensitive metal detector to ensure food and drug safety. Several detection methods currently exist, such as eddy current detectors, x-ray imaging, and systems based on superconducting quantum interference devices (SQUIDs). The eddy current method is widely used; however, the sensitivity is highly affected by the conductivity of the contaminants and the food itself. Since wires of strainer elements or syringe needles are made of stainless steel, their conductivities are lower than carbon steel, making them difficult to detect using the eddy current method. The x-ray method is a useful technique and is increasingly popular in food factories, and it can detect both metal and nonmetallic contaminants. However, maintenance costs for x-ray equipment are high, and the lower detection limit for practical x-ray usage is of the order of 1 mm. Along with others, the authors have proposed the development of a detection system using a SQUID magnetic sensor to circumvent the difficulties outlined above [1–5]. The detection technique is based on recording the remanent magnetic field of contaminant by SQUID sensors. Here we describe a contaminant detection system for food contaminants with a robust magnetically shielded box.

2. Principle

A block diagram of the detection system is shown in figure 1. It consists of a permanent magnet, a conveyor, a magnetically shielded box, and a SQUID sensor. All of the samples move from left to right and pass through the magnet tunnel before

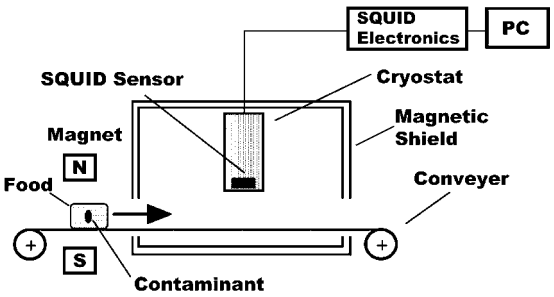

Figure 1. Block diagram of food contaminant detection system. The system consists of a permanent magnet, a conveyor, a magnetically shielded box, and SQUIDs.

detection. An austenitic stainless steel material is originally nonmagnetic. However, it shows properties similar to those of a ferromagnetic material after martensitic transformation during its fabrication [6]. Therefore the magnetization prior to the detection is also effective for austenitic stainless steel contaminants. The remanent magnetic field from a metallic contaminant in food is detected by the SQUID magnetometers when it passes below the sensor.

3. System

3.1. General specification

The size of the whole system (length × width × height) is 1500 mm × 477 mm × 1445 mm; it is covered with stainless steel, and approvable under HACCP (Hazard Analysis and Critical Control Point) guidelines. The magnet is made of Nd base alloy and its magnetic field is 0.1 T. The liquid nitrogen (LN_2) cryostat used for maintaining the temperature of the SQUIDs at 77 K consists of three separated glass Dewars. The size of each Dewar is 70 mm O.D. × 50 mm I.D. × 300 mm in length. The total volume of the cryostat is 1.5 l and the liquid nitrogen can be maintained for 12 h without filling. An automatic LN_2 supply system is attached. Three high-T_c SQUIDs are installed in this system. The SQUID and its driving electronics employed here were manufactured by Sumitomo Electric Hightechs [7]. The size of the pickup loop is 10 mm × 10 mm square and it is of the high-T_c directly coupled type. The sensitivity of the SQUID is nominally 300 fT $Hz^{-1/2}$ at 10 Hz. The SQUID driving electronics are of modulation type with a bandwidth of 10 kHz. The signal is passed through a low-pass filter (LPF) at a cutoff frequency of 5 Hz. The system is totally controlled by a PC and can be operated by touching the display panel in front of the system. All the electronics except for the PC and the glass Dewars with SQUIDs are surrounded by aluminium shield panels which prevent electromagnetic disturbance outside the system. The appearance of the system is shown in figure 2 [8].

3.2. Magnetic shield design

Since the magnetic shield covering the sensors is the crucial part of the system for practical use, special attention was given to its design. Prior to system design, 3D analyses of the magnetic field distribution inside the magnetic shield were carried out.

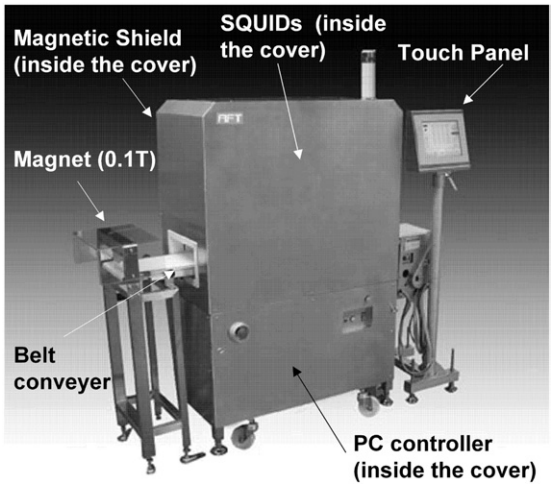

Figure 2. Appearance of the complete system. The size of the system (L × W × H) is 1500 mm × 477 mm × 1445 mm, and it is covered with stainless steel, which is approvable under the HACCP (Hazard Analysis and Critical Control Point) guidelines.

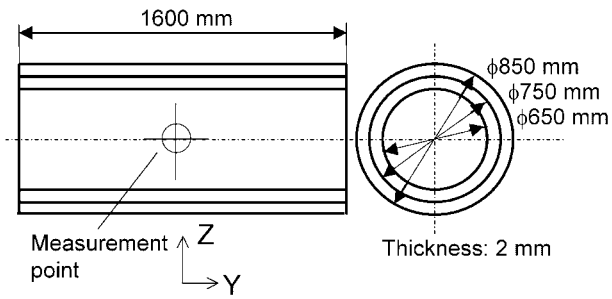

Figure 3. Simple tri-layered cylindrical magnetic shield model for finite element method (FEM) simulation. The shield dimensions are ϕ850 mm × ϕ750 mm × ϕ650 mm × 1600L mm. Thickness of the material is 2 mm.

First, a finite element model (FEM) simulation was performed on a PC for the simple tri-layered cylindrical magnetic shield model shown in figure 3. The model dimensions were ϕ850 mm × ϕ750 mm × ϕ650 mm × 1600L mm. The thickness of the material was 2 mm. The simulation software Maxwell (*Ansoft Corporation*, Japan) was used. A dc magnetic field of 5.3 μT was applied along the Z-direction and the field distribution inside the shield was calculated as a function of the relative permeability μ_s of the material. The shielding factor (SF) was calculated as a ratio of the imposed external magnetic induction to the value of the magnetic induction at the centre of the internal region of the shield. Figure 4 shows the dependence of the SF on the relative permeability. It indicates that the SF increases linearly with relative permeability μ_s. An actual tri-layered cylindrical magnetic shield, having the same dimensions as the model described above, was then built using permalloy. The SF of this shield was obtained by applying a dc field of 5.3 μT; the SF was found to be 1250 at the centre of the cylinder. We thus estimate the relative permeability of the material to be about 20 000 by comparing the value shown in figure 4.

Second, a rectangular shape model as shown in figure 5, which is more realistic and suitable for our system, was

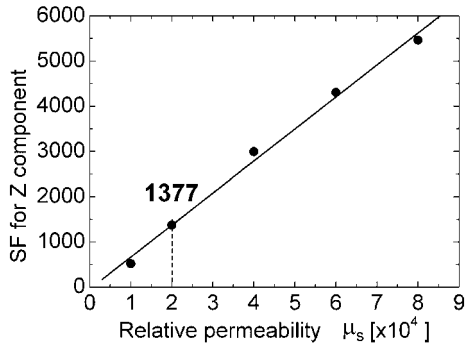

Figure 4. Dependence of the SF on the relative permeability. The SF was found to increase linearly along the relative permeability μ_s.

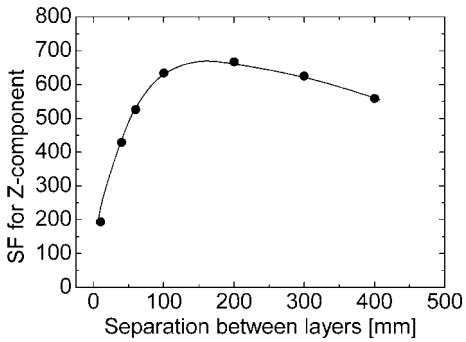

Figure 6. Shielding factor as a function of layer separation. The SF presents a nonlinear behaviour with a maximum at around the layer separation of 100–200 mm.

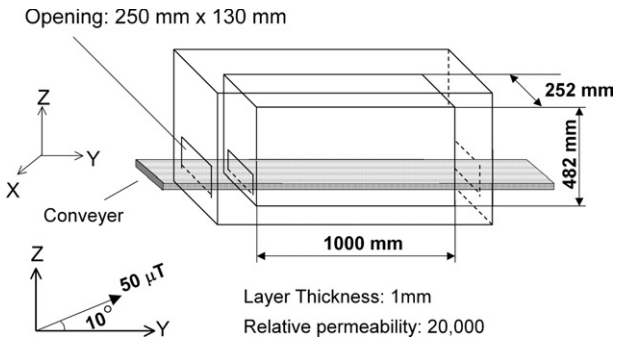

Figure 5. Rectangular shape model for FEM simulation. This model is more realistic and suitable for the system. Two shield layers are used. The size of the inner shield box is fixed (1000 mm × 252 mm × 482 mm, L × W × H); the spacing between inner and outer boxes is changed from 10 to 400 mm.

employed for the simulation. Two shield layers were used. The same software was used for the FEM simulation. A magnetic field of 50 μT was applied along the Y-direction with an angle of 10°. The thickness of the permalloy layer and the relative permeability were assumed to be 1 mm and 20 000, respectively. The size of the inner shield box was fixed at 1000 mm in length, 252 mm in width, and 482 mm in height; the spacing between the inner and outer boxes was changed from 10 to 400 mm [9]. The shielding factor SF was calculated in the same manner as for the cylindrical case. Figure 6 shows the shielding factor calculated as the ratio between the Z-component of the magnetic field outside and at the centre of the shield (z = 140 mm from the bottom of the inner shield box). The shielding factor presents a nonlinear behaviour and a maximum at around the layer separation of 100–200 mm. Due to material cost considerations, a separation distance of 100 mm was selected for the shield box design. In this model a shielding factor SF of 634 was obtained.

The shielding factor was then analysed in the same manner when the length Y of the inner shield was shortened to 700 mm and the height was extended to 532 mm; an SF of 523 was obtained, which is high enough for practical use. The final dimensions of the inner shield (L × W × H) were set at 700 mm × 252 mm × 532H mm, while the outer shield was 902 mm × 454 mm × 734 mm.

4. Characterization of the system

The double-layered shield box described above was fabricated. Then the actual shielding factor of the shield box was evaluated by applying a dc magnetic field. An SF value of 732 was obtained, which was 40% larger than the calculated value. This suggests that the relative permeability of the shield materials was higher than the value we expected because it is dependent on the annealing conditions.

The performance of the total system was tested. Steel balls and stainless steel balls with different diameters were prepared as test samples. The samples were put on the conveyer and magnetized. Then they were passed below the SQUIDs with a speed of 14 m min^{-1}. Figure 7 shows the time traces of the signals from a SQUID located above the middle of the conveyor. The signals were recorded when each stainless steel ball (sus304) with a diameter of 0.3 and 0.6 mm passed through the device just under the SQUID with a separation of 75 mm. A conversion factor (volt to tesla) of 1.2 nT V^{-1} was used. Clear signals with signal-to-noise (S/N) ratios of more than 4 were obtained. The signal was not affected by either electromagnetic radiation of a nearby mobile phone or the motion of a bulky steel cart near the system. Figure 8 shows the dependence of the SQUID output peak signal on the sample diameter. For steel balls (solid circle), the signals scaled well with the cube of the diameter. This suggests that the signal is proportional to the volume of each sample. In contrast, stainless steel balls (open circles), which are nominally austenitic stainless, produced signals which deviated from expected values because their magnetism depends on the martensitic phase content which is affected by the mechanical history of the material [5].

It was demonstrated that the system can successfully find a stainless steel ball as small as 0.3 mm in diameter. However, we note that it may be difficult to find a contaminant in food which contains large amounts of iron, such as blueberries, seaweeds, and chocolates, because the magnetic signal of the contaminant becomes comparable to that of the food.

5. Conclusion

We have designed and constructed a food contaminant detection system using high-T_c SQUID magnetometers. The

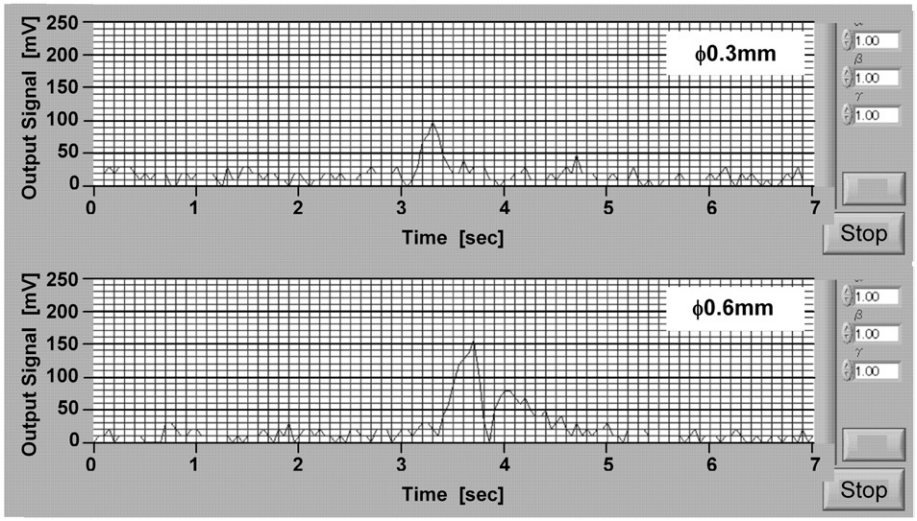

Figure 7. Time traces of the signals from a SQUID located in the centre. They were recorded when each stainless steel ball (sus304) with a diameter of 0.3 mm and 0.6 mm passed through the device just under the SQUID with a separation of 75 mm. The conversion factor of volt to tesla is 1.2 nT V^{-1}.

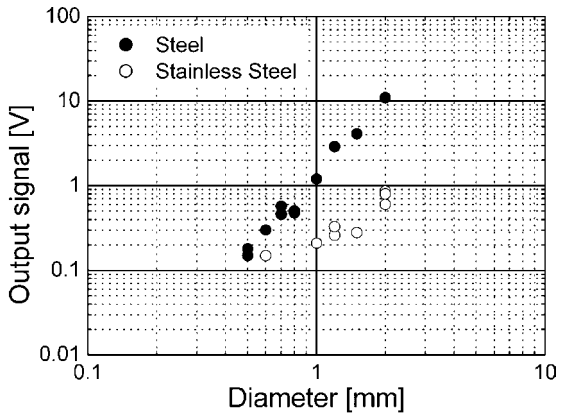

Figure 8. Dependence of the SQUID output peak signal on the sample diameter. For steel balls (solid circles), the signals scaled well with the cube of the diameter. In contrast, the signals obtained from stainless steel balls (open circles), deviated from expected values.

detection technique is based on recording the remanent magnetic field of a contaminant using SQUID sensors. The magnetic shield which covers the SQUID sensors was designed carefully because it is a crucial part of the system for practical use. After the FEM simulation, a double-layered rectangular magnetic shield using permalloy metal was made with a shielding factor SF of 732. Spherical stainless steel test balls as small as 0.3 mm in diameter were successfully detected with an S/N ratio higher than 4. The system was robust and was not affected by the disturbance of electromagnetic waves generated by a mobile phone or the motion of nearby iron objects.

Acknowledgments

This work was supported in part by the Cooperation of Innovative Technology and Advanced Research in Evolutional Area, and by the 21st Century COE Program 'Ecological Engineering for Homeostatic Human Activities' from the Ministry of Education, Culture, Sports, Science, and Technology.

References

[1] Tanaka S 2005 *IEICE Trans. Electron.* C **88** 175–9
[2] Tanaka S 2004 *Supercond. Sci. Technol.* **17** 620–3
[3] Bick M 2003 *ISEC03: 9th Int. Superconductive Electronics Conf. PTh06* (Extended abstracts)
[4] Donaldson G B, Cochran A and McKirdy D 1996 *Fundamentals and Applications* ed H Weinstock (New York: Kluwer–Academic) p 599
[5] Krause H 2005 *IEEE Trans. Appl. Supercond.* **15** 745–8
[6] Huang H 1996 *Mater. Sci. Eng.* A **216** 178–84
[7] Available online http://www.shs.co.jp/squid/
[8] Available online http://www.aftweb.co.jp/squid/index.htm
[9] Fauri M 1990 *IEEE Trans. Magn.* **26** 364–7